High carbon mineralization rates in subseafloor hadal sediments - Result of frequent mass wasting

M. Zabel[1], R. N. Glud[2,3], H. Sanei[4], M. Elvert[1,5], T. Pape[5], P.-C. Chuang[6], E. Okuma[5], P. Geprägs[1], M. Kölling[1]

[1] MARUM – Center for Marine Environmental Science, University of Bremen, Leobener Str. 8, 28359 Bremen, Germany

[2] Hadal & Nordcee, Department of Biology, University of Southern Denmark, Campusvej 55, 5230 Odense, Denmark

[3] Tokyo University of Marine Science and Technology, 4-5-7 Konan, Minato-ku, Tokyo, 108-8477, Japan

[4] Lithospheric Organic Carbon (LOC) Group, Department of Geoscience, Aarhus University, Høegh-Guldbergs gade 2, 8000C, Aarhus, Denmark

[5] Faculty of Geosciences, University of Bremen, Klagenfurter Str. 2-4, 28359 Bremen, Germany

[6] GEOMAR Helmholtz Centre for Ocean Research, Wischhofstr. 1-3, 24148 Kiel, Germany

Corresponding author: Matthias Zabel (mzabel@uni-bremen.de)

Key Points:

- Hadal subseafloor pore water profiles from the Japan Trench and Atacama Trench document unexpectedly high microbial turnover rates.
- Frequent alternations between hemipelagic sedimentation and mass wasting lead to high burial efficiency of reactive organic carbon.
- Microbial activities in deep-sea trenches may be similar to those at the edge of high-production areas.

Abstract

In the past 20 years, the exploration of deep ocean trenches has led to spectacular new insights. Even in the deepest canyons, an unusual variety of life and unexpectedly high benthic oxygen consumption rates have been detected while microbial processes below the surface of the hadal seafloor remains largely unknown. The information that exist comes from geophysical measurements, especially related to seismic research, and specific component analyses to estimate the carbon export. In contrast, no information is available on metabolic activities in deeper buried sediments of hadal environment. Here we present the first pore water profiles from 15 up to 11 m long sediment cores recovered during three expeditions to two hadal zones, the Japan Trench and the Atacama Trench. Despite low levels of organic debris, our data reveal that rates of microbial carbon turnover along the trench axes can be similar to those encountered in much shallower and more productive oceanic regions. The extreme sedimentation dynamics, characterized by frequent mass wasting of slope sediments into

the trenches, result in effective burial of reactive, microbially available, organic material. Our results document the fueling of the deep hadal biosphere with bioavailable material and thus provide important understanding on the function of deep-sea trenches and the hadal carbon cycle.

Plain Language Summary

For a long time, it was assumed that in water depths below 6,000m, biological species diversity and microbial activity is very low. Recent studies could already provide clear evidence that significant degradation of organic material occurs even at the seafloor surface in deep-sea trenches. No comparable information is available yet about the situation below the surface layer. Here, data are presented for the first time that help to close this knowledge gap. Based on geochemical parameters, it can be proven that very active degradation processes also take place in the deeper buried layers in deep-sea trenches. Rates correspond in magnitude to sediments from shallower water depths with considerably higher contents of organic material. The authors attribute this finding primarily to sedimentation dynamics in deep-sea trenches. The steep flanks of trenches, sometimes associated with seismic activity, repeatedly favor the sliding of large sediment packages into basins along trench axes. Rapid burial removes less degraded, and thus more microbially available material from oxic surface and preserves it for subsequent processes such as sulfate reduction. The unique results provide important new insights into the function of deep-sea trenches and the hadal carbon cycle.

1 Introduction

Only recently it has been realized that hadal trenches harbor a surprisingly high biological activity (Danovaro et al., 2003; Bartlett, 2009; Jamison, 2015). In situ measurements have documented that microbial oxygen depletion at the seafloor surface in deep sea trenches is far more efficient than would be expected at such great water depths (Glud et al., 2013; Wenzhöfer et al., 2016; Luo et al., 2018). These findings suggest that the input of degradable material must be considerably greater than estimated assuming purely vertical transport from the euphotic zone either driven by hydrographic and/or down slope funneling of material or by mass wasting (Oguri et al., 2011; Turnewitsch et al., 2014; Ichino et al., 2015; van Haren, 2020).

There are several recent studies of the impact and frequency of seismically triggered submarine landslides. Especially, the devastating Tohoku-Oki earthquake in the Japan Trench in 2011 has led to a series of papers on the relationship between seismic activity and sedimentation processes in trench systems (e.g., Strasser et al., 2013; Ikehara et al., 2016; McHugh et al., 2016; Luo, et al., 2017; Bao et al., 2018; Kioka et al., 2019a/b; Ikehara et al., 2020). All these advances clearly document that sedimentation at the trench axes is massively influenced by mobilization and redeposition of sediments from the lateral trench flanks. The obvious influence of these sedimentation processes on the flux of organic carbon and its balances could also be demonstrated (Luo et al., 2017;

Kioka et al., 2019b). However, previous studies on subseafloor sediments in hadal trenches are mainly based on sediment-acoustic profiles and analyses of the sedimentary solid phase, while the pore fluids have stayed almost unstudied. In contrast to other ocean regions where pore water investigations in subseafloor sediments were used to decipher the processes of the deep biosphere more than 2.4 km below the seafloor (e.g., Inagaki et al., 2015; Heuer et al., 2020), to our knowledge, only two classic pore water profiles from subsurface sediments have been published to date from water depths >7,000 m (Strasser et al., 2013) . Without any biogeochemical interpretation, both partial sulfate profiles were used to document a recent mass displacement event only. Furthermore, only two studies exist to date with data from deep-sea trenches that contain pore water information from a maximum depth of 30cm below the seafloor (Glud et al. 2013, 2021; Thamdrup et al. 2021).

In this study, we present geochemical data from 15 up to 11 m long sediment cores recovered from hadal trenches off Japan and Chile at maximum water depths of 8,025 m and 7,996 m, respectively. The data are used to document elevated indicators for metabolic activities in subseafloor hadal sediments and discuss the potential importance for element cycling and organic carbon retention in deep sea trenches.

2 Study areas

The Japan Trench is the product of subduction of the Pacific Plate in the East under the Okhotsk Plate in the West (Fig. 1A). The convergence rate is 7-9 cm yr^{-1} (Loveless & Meade, 2010, McHugh et al., 2020). The trench is about 800 km long and reaches a maximum water depth of about 8,400 m.

The Atacama Trench, a section of the Peru-Chile Trench, is located in the south-eastern Pacific (Fig. 1B). Formation of the trench is caused by the subduction of the oceanic Nazca Plate underneath the South American Plate on a length of about 6,000 km. The convergence is estimated to be up to 7 cm yr^{-1}, (Angermann et al., 1999) and the dip of the subducting plate is 10° (Contreras-Reyes et al., 2012). At its deepest point the water depth is almost 8,100 m.

Primarily due to plate movement, associated seismic activity, fault structures and flexural bending of the oceanic plates, both trench axes in particular are often fractured and characterized by isolated trench-fill and graben-fill basins (Geersen et al., 2018a, b; Kioka et al., 2019a). The sediments in both trenches mostly consist of interbedded strata of turbiditic and hemipelagic origin (e.g., Ikehara et al. 2016; Bao et al., 2018). The remobilization of sediments on continental slopes and thus deposition of turbidite sequences in trench axes are usually seismically triggered. Most recent examples are the M_W9.0 Tohoku-Oki earthquake 2011 offshore Japan (Yokota et al., 2011; Strasser et al., 2013; McHugh et al. 2020) and the M_W8.1 Iquique earthquake in northern Chile (Schurr et al., 2014). Both events led to corresponding sediment redistributions towards the trench axes.

3 Material and Methods

3.1 Sampling

Sediment and pore water samples for this study were collected in the Japan Trench and the Atacama Trench regions during three expeditions with the German deep-sea research vessels SONNE (old) and SONNE (new) (Fig. 1, Table 1). The Japan Trench expeditions took place in 2012 (SO219A, core code GeoB164xx; Wefer et al., 2014) and 2016 (SO251, core code GeoB218xx; Strasser et al., 2017). Samples from the Atacama Trench were collected in 2018 (SO261, core code GeoB229xx; Wenzhöfer et al., 2019). A piston corer was used for sediment sampling on cruise SO251, while a gravity corer and a multiple core were used on the other two cruises. Here we provide a subset of data from 17 different sites, 11 sites located in the Japan Trench region and 6 in the Atacama Trench region. 12 cores have been recovered from the Trench axes, 4 from the slopes and one core originates from the edge to the abyssal plain in the Chile Basin. Pore water analyses were conducted on all recovered sediment cores, while more specialized investigations only were performed on some selected sediment samples.

Syringe (headspace) samples for gas analytics (0.5-5 ml sediment in 4-20 ml vials with a 2 mL saturated NaCl brine receiver) were taken immediately after sediment recovery on the work deck instantaneously after cutting the cores into sections. The extraction of pore water samples was performed on closed 1 m-whole round core sections within the first three hours after core recovery by drilling small holes in the plastic liners and inserting Rhizon Micro Suction Samplers (Dickens et al., 2007). Subsamples for XRF analysis, radiocarbon dating on total organic carbon (TOC) and composition of organic material were taken onshore after the cruises in the core repository at the MARUM, Univ. of Bremen, where all sediment cores have been stored at 4°C (https://www.marum.de/en/Infrastructure/MARUM-GeoB-Core-Repository.html).

3.2 Pore water and dissolved gas analyses

Some of the analyses used for this study were already carried out offshore. These include alkalinity titration, pH measurement, and the analysis of ammonium (SO219, SO261) and iron (only SO261).

Alkalinity has been analyzed by gran titration of known quantities of pore water sample by addition of HCl on a micro stirring device. The accuracy of this method was better than 0.2 mM (data not shown). Dissolved iron (Fe^{2+}) concentrations were analyzed photometrically at wavelength of 565 nm with a Hach Lange DR 2800 Photometer following the method of Collins et al. (1959). Dissolved ammonium (NH_4^+) was detected using the PTFE tape gas separator technique (modified after Hall and Aller 1992). Dissolved Manganese concentrations were analyzed in acidified samples with an inductively coupled plasma optical emission spectrometer (ICP-OES; Varian Vista PRO). The precision was better than 3 % with a detection limit of 0.04 µM. Sulfate (SO_4^{2-}) concentrations were determined by ion chromatography (Metrohm 861 Advanced Compact IC,

Metrohm A Supp 5 column, 0.8 mL min^{-1}, conductivity detection after chemical suppression) in samples diluted 1:40 with Milli-Q-grade H_2O. Dissolved methane (CH_4) concentrations were analysed following the headspace method described by Kvenvolden (1986) and D'Hondt et al. (2003). For samples from the Japan Trench we used an Agilent Technologies 6890N gas chromatograph equipped with a flame ionization detector (Pape et al., 2010), while samples from Atacama Trench site GeoB22908/A10 a ThermoFinnigan Trace gas chromatograph equipped with a flame ionization detector and a Carboxen-1006 PLOT fused-silica capillary column (0.32 mm by 30 m; Supelco, Inc., USA) was used. The stable carbon isotopic composition of methane in four samples from the Atacama trench was determined by duplicate analysis using a Trace GC Ultra coupled to a Delta Plus XP isotope ratio mass spectrometer via a GC Combustion III interface (all ThermoFinnigan; Zhuang et al., 2018). Information on the calculation of flux rates are given in the supplements.

3.3 Sediment analyses

Solid phase iron and manganese concentrations is sediments of core GeoB22908-2(A10) were measured using the high-resolution (1 cm) semi-quantitative XRF (X-ray fluorescence) Avaatech at MARUM, performed with an excitation potential of 10 kV, a current of 250 mA and 30 s counting time. Scans were calibrated with quantitative XRF measurements on discrete samples using a PANalytical Epsilon3-XL XRF spectrometer equipped with a rhodium tube, several filters and an SSD5 detector and certified standard materials (e.g., GBW07309, GBW07316 and MAG-1). Scans of the bulk (Gamma Ray) density were conducted with a Multi-Sensor Core Logger (MSCL; GEOTEK®) at MARUM. The MSCL was equipped with a line scan camera for high-resolution core image acquisition.

3.4 Organic fraction measurements

Accelerator Mass Spectrometry measurements (AMS) of radiocarbon (^{14}C) ages on TOC of samples from core GeoB22908-1 were carried out in the MICADAS radiocarbon laboratory at Alfred-Wegener Institute (AWI), Germany (cf. Supplementary Table S1). ^{14}C bulk ages are uncalibrated.

A programmed pyrolysis method (Hawk instrument, Wildcat Technologies, USA) at the Lithospheric Organic Carbon Lab (LOC) of the Department of Geoscience, Aarhus University, was used to measure TOC and the reactive organic carbon content. In this method, 50 mg dry sample is subject to a two-step, programmed pyrolysis and oxidation heating cycle. During the pyrolysis step, the sample is heated to an iso-temperature of 300°C for 3 minutes and then ramped up (25°C min^{-1}) to 650°C. All hydrocarbons and organic-derived fractions of CO, and CO_2 are summed up as the reactive organic carbon content. The sample is then subject to oxidative heating, which releases the residual organically-derived CO and CO_2. The sum of the reactive organic carbon and residual organic carbon is equivalent to TOC.

C/N values in the Atacama trench core GeoB22908-2(A10) were analyzed from

freeze-dried homogenized sediment of each sampling interval. In brief, 3 g of the sediment was decalcified by the addition of 10 % HCl followed by repetitive washing steps with ultrapure water. For C/N determination, 10–30 mg of the dried sediment was weighed into tin capsules and analyzed via a Thermo Scientific Flash 2000 elemental analyzer connected to a Thermo Scientific Delta V Plus IRMS.

4 Results

In 9 of the 12 sediment cores from the trench axes, pore water sulfate concentrations exhibited steep declines towards the sulfate-methane transition zone (SMT) which was encountered between 350 cm and 950 cm below the seafloor (Figs. 2) with standard gravity coring / piston coring equipment. Consistently ammonium concentrations increase up to 4 mM (GeoB16431-1) and values for alkalinity reached remarkable 71.3 $mM_{(eq)}$ (GeoB21817-1) below the SMT. In the cores, where sulfate was completely depleted within the core length, increasing methane concentrations have been determined below (Figs. 2). Only at three sites in the Atacama trench (GeoB22902-1/A6, 22905-2/A3, 22907-2/A2), the diagenetic activity was apparently lower. Cores did not penetrate the SMT and the increases of NH_4^+ concentrations and alkalinities are relatively weak (Fig. S1). All cores from the four slope sites (GeoB16442-1, 21810-1, 21815-1, 22909-1/A9) and the abyssal site (GeoB22906-/A7) also reveal comparably low rates of early diagenetic activity (Fig. 3).

For the cores from the Japan Trench, several publications have already presented and discussed frequent changes between seismically induced mass wasting and layers of "normal" sedimentation (Strasser et al., 2013; Ikehara et al., 2016; Boa et al., 2018; Kioka et al., 2019a, 2019b; Schwestermann et al., 2020). Based on AMS^{14}C dating, some of the mass wasting events could be attributed to historical seismic activities. The cores from the Atacama Trench, presented for the first time in this study, also show such alternating deposits as indicated by physical and geochemical sediment property data. As an example, Fig. 4 shows the density record in core GeoB22908/A10, which shows the typical signatures of intercalations of hemipelagic sedimentation with turbidite layers. Additionally, AMS^{14}C ages and strong, sharply defined enrichments of redox-sensitive elements Fe and Mn clearly indicate intensifications of redox processes caused by mass wasting events (McHugh et al., 2011, 2016; Polonia et al. 2013).

A particularly prominent section of core GeoB22908/A10 that shows the effects of intercalated turbidite layers very well is shown in Figure 5. Above about 285 cm sediment depth, both density and magnetic susceptibility increase abruptly. A sharp Mn peak is formed at the lower edge of this transition. Fe is also clearly enriched, but the boundaries are more gradual.

The organic fraction also shows a difference between the sediment units. This concerns both the quantity (Fig. 5D) and the composition of the organic material (Fig. 5E). In the turbiditic layers (top and bottom), the TOC contents are significantly lower than in the interbedded, "normal" sediments. The same

applies to the proportion of reactive organic carbon in the TOC. The C/N ratio is significantly lower at the lower edge of the turbiditic sequence and at the surface of the "normal" sediments, respectively.

5 Discussion

5.1 Classification of the pore water profiles

Although in situ measurements of microbial oxygen consumption at the surface of sediments in deep-sea trenches already revealed surprisingly high rates (Glud et al., 2013, 2021; Wenzhöfer et al., 2016), the high intensities of the turnover rates in subseafloor sediment as reflected by the shallow SMT, were rather unexpected (Fig. 6A). The special nature of the sediments in the trench-fill basins becomes clear, when the diffusive flux rates of SO_4^{2-} and CH_4 are compared with rates reported in studies using compilations of global data sets. In Table 2 SO_4^{2-} and CH_4 flux rates of all sediment cores are listed along with average rates from ocean depth regions. Comparing the SO_4^{2-} fluxes from the trench cores (Japan Trench: up to 0.132 mmol $m^{-2}d^{-1}$; Atacama Trench: up to 0.148 mmol $m^{-2}d^{-1}$) to global average data as documented by Egger et al. (2018), the trench SO_4^{2-} fluxes are similar to outer shelf (cf. Niggemann et al., 2007), or upper to middle continental slope values, but far from data estimated for a water depth of >7,500 m. In both trenches, SO_4^{2-} fluxes are significantly higher in the trench axes than on the respective flanks (Fig. 6B). This also applies to the three sites in the Atacama Trench where the SMT was not reached. Interestingly, the pore water data from the Japan Trench suggests that on the slopes above the hadal zone (<6,000 m) the common relationship between decreasing SO_4^{2-} flux rates with increasing water depth appears to hold (Fig. 6B).

Most research to date has found close correlations between TOC content, water depth, and SMT depth (e.g. Bowles et al., 2016; Egger et al., 2018). The rationale being that the greater the water depth, the lower the input of degradable organic material and the lower the intensity of early-diagenetic degradation processes. TOC concentrations in sediments at locations in the two trenches are slightly elevated compared to those at abyssal plains (e.g. Xu et al., 2021), but far from known TOC-rich deposits (e.g., Inthorn et al., 2006; Seiter et al., 2004). As an example, despite a 6-fold lower TOC content at the trench sites than in sediments recovered from the slope off Namibia (Riedinger et al., 2006), SO_4^{-2}, CH_4 and alkalinity profiles are very similar (Fig. S2). It appears that the quantity of TOC alone is not the only factor controlling high intensity of microbial turnover rates in subseafloor sediments in hadal trenches.

5.2 Importance of the sedimentation regime

The apparent inconsistency of low TOC levels and high microbial activity in the subsurface hadal sediment suggests that the unique sedimentation regime in deep-sea trenches must have a significant impact on biogeochemical processes below the seafloor. In contrast to regions with continuous, vertical sedimentation from the productive surface ocean (like in the example of Fig. S2), the trench axes frequently receive mass wasting deposits. The radio carbon ages in

the core GeoB22908-2(A10) indicate that the deposition of the thick turbidite between 165 cmbsf and 280 cmbsf may be triggered by the recently described 3.8 kyr old mega earthquake in the region (Salazar et al., 2022).

Figure 5 shows a typical section from the Atacama Trench core GeoB22908-2(A10) in detail. Based on the high-resolution density and magnetic susceptibility profiles and two radiocarbon ages, hemipelagic, "normal" sediments can be clearly identified sandwiched between two turbidite layers. Also, the typical enrichments of manganese (and iron) clearly indicate sudden changes in the geochemical environment as triggered by massive changes in sedimentation conditions (McHugh et al., 2011, 2016; Polonia et al 2013; Figs. 5C). The significantly lower TOC content and the relatively higher C/N ratio of the redeposited sediment classify both sediment layers above and below as pre-aged and pre-degraded (Fig. 5D; cf. Wakeham, 2002). However, this does not mean that redeposited material can always be characterized in this way. Bao et al. (2018) and Kioka et al. (2019b) show that remobilized sediments need not be significantly older or poorer in TOC than the hemipelagic sections. In sediment core GeoB16431-1 (Figs. 1, 2) different sediment compositions occur with different turbidite layers. Ultimately, the primary depositional site and the age of remobilized sediments may determine their TOC content and its composition (cf. Schwestermann et al., 2021). The presented section of core GeoB22908-2(A10) provide such an example with significantly higher reactive organic carbon contents in the intermediate hemipelagic sediments (Fig. 5E). Overall the reactivity of the deposited organic material correlates well with the age of the material (Fig. 7), but not necessarily with the sediment depth. Thus, the two oldest samples in core GeoB22908-2(A10), which were taken from the upper, massive turbidite layer displayed in Fig. 5, show significantly lower contents of reactive TOC components than samples with younger ^{14}C ages from "normal", hemipelagic sediments at depths of 122 cm and 533 cm (Table S1).

From the age of the surface sediments at site GeoB22908/A10 (2.99 kyr; Xu et al., 2021) and the age of the deepest dated sample in the corresponding long core (8.03 kyr at 615 cmbsf; cf. Table S1) a total sedimentation rate (SR) of 122 cm kyr^{-1} may be estimated if all turbidite layers are included in the sediment thickness. Incidentally, this rate is in the same order of magnitude as published total SR in basins along the Japan Trench (Ikehara et al., 2016). Based on AMS$^{14}C_{TOC}$ from samples of a multiple corer core recovered at the same site (uppermost 35 cm), Xu et al. (2021) calculated a SR of 27 cm kyr^{-1} for what appears to be predominantly hemipelagic sediments. For comparison only, this near-surface estimate is only 3-4 times smaller than calculations on the adjacent shelf (Muñoz et al., 2004), but more than 20 times higher than calculated for the surface sediments at the nearby rise site GeoB22909/A9 (cf. Fig. 1; Xu et al., 2021). The ratio of the various SRs (as well as corresponding $^{210}Pb_{ex}$ profile; (Oguri et al., in rev.) allows the assumption that the uppermost 6 m of sediment at site GeoB22908/A10 consist of about 80 % redeposited, pre-aged and pre-degraded material. Despite all the known uncertainties in determining reliable age of marine sediments, this rough estimate indicates that

sedimentation dynamics in deep-sea trenches should be of great importance for the specific biogeochemical activity through out the deposited sediment.

The rationale of this approach applied to site GeoB22908/A10 becomes even more obvious if available analytical data are used in a simple mass balance. On the basis of microelectrode measurements, Glud et al. (2021) determined the in-situ penetration depth of oxygen as 3.1 cm and calculated a diffusive oxygen uptake (DOU) of 1.5 mM $m^{-2}d^{-1}$, considering an 8 % fraction of inorganic oxidation processes. Depending on the stoichiometry of oxic respiration (CH_2O:O_2 = 1:1; for Redfield org. matter = 1:0.77), this oxygen consumption corresponds to a microbially transformed amount of organic carbon of 14-18 mg $C_{org.}$ $m^{-2}d^{-1}$. Assuming a porosity of 85 %, a dry bulk density (DBD) of 0.41 g ccm^{-1} and an average TOC mass fraction of 1.5 wt% (Xu et al., 2021), the oxic layer contains about 188 g $C_{org.}$ m^{-2}. If the oxygen concentration profiles would represent steady-state conditions and the oxic layer would have been accumulated in 111 yrs (3.1 cm O_2 penetration depth / 27 cm kyr^{-1} SR), DOU would correspond to 563-732 g degraded $C_{org.}$ m^{-2} during this time. Considering that 188 g C_{org} m^{-2} are available, the estimated time period is by far too long. Alternatively, if we use the total SR (122 cm kyr^{-1}) this would result in a principally possible quantity of 128-167 g C_{org} m^{-2}. However, since only a fraction of TOC is microbially degradable, even the assumption of a 27-year passage through the oxic zone seems too long. Therefore, the most obvious conclusion for bringing all existing data in line is that the time for oxidative degradation of organic material must have been significantly shorter.

Apart from the fact that the assumption of stationary conditions is certainly not correct, especially for hadal regimes, our assessment strongly suggests that the burial efficiency of organic material is key to the understanding of the biogeochemistry in such systems. Mass deposition events of C_{org}-poor and less reactive sediment layers deprive previous, C_{org}-rich surface sediments of oxic degradation. Labile, microbially degradable components are buried and become subject to subsequent processes of early diagenetic succession, especially via sulfate reduction.

It becomes obvious that the bulk TOC content alone cannot be used as a proxy for the intensity of biogeochemical processing in subseafloor sediments of trench systems, but that the age and source of the material is important for the microbial driven diagenesis. Thus, the frequency and thickness of turbiditic deposits are of great importance for resolving the mineralization and burial efficiency of organic material in hadal sediments.

6 Conclusions

Pore water data from subseafloor sediments at the Japan Trench and Atacama Trench reveal that high rates of organic matter degradation processes are not restricted to shallow water depths or hadal surface layers. Despite low to moderate levels of organic carbon content, diagenetic process rates at depths of several meters below the seafloor are comparable with data and fluxes from much shal-

lower, more productive oceanic regions. Our study add to the insights gained from surface sediments. The general correlation between mineralization rates, water depth or TOC content does not apply in trench systems. Due to the small areal contribution of the hadal zone to the total area of marine deposits, the findings may have a minor effect on global estimates of organic carbon degradation rates. However, they provide essential new insights for hiving thorough understanding of element cycling, microbial processing and microbial community structures in these highly dynamic systems and the depot center function of deep-sea trenches.

Declaration of competing interest

The authors declare that they have no known competing financial interests or personal relationships that could have appeared to influence the work reported in this paper.

Acknowledgements

We acknowledge the captains and crews of the RV SONNE cruises SO219, SO251 and SO261M123 and the respective chief scientists G. Wefer (MARUM), M. Strasser (Univ. of Innsbruck and F. Wenzhöfer (Max Planck Inst. for Marine Microbiology, Bremen). Special thanks belong to S. Pape, N. Lübben and J. Malnati (all Faculty of Geoscience, Univ. of Bremen) for their great assistance in the labs. Financial support was provided by HADES-ERC Advanced grant "Benthic diagenesis and microbiology of hadal trenches" #669947, the Danish National Research Foundation grant DNRF145 (Danish Center for Hadal Research) and Deutsche Forschungsgemeinschaft (DFG, German Research Foundation) under Germany's Excellence Initiative/Strategy through the Clusters of Excellence "The Ocean in the Earth System" (EXC 309–49926684).

References Angermann, D., Klotz, J., & Reigber, C. (1999). Space-geodetic estimation of the Nazca-South America Euler vector. *Earth and Planetary Science Letters,171,* 329-334. doi: 10.1016/S0012-821X(99)00173-9

Bao, R., Strasser, M., McNichol, A. P., Haghipour, N., McIntyre, C., Wefer, G., & Eglinton, T.I. (2018). Tectonically-triggered sediment and carbon export to the Hadal zone. *Nature Communications, 9,* 121. doi: 10.1038/s41467-017-02504-1

Bartlett, D. H. (2009). Microbial life in the trenches. *Marine Technology Society Journal, 43,* 128–131. doi: 10.4031/MTSJ.43.5.5

Bowles, M. W., Mogollón, J. M., Kasten, S., Zabel, M., & Hinrichs, K.-U. (2014). Global rates of marine sulfate reduction and implications for sub-sea-floor metabolic activities. *Science, 344,* 889-891. doi: 10.1126/science.1249213

Collins, P. F., Diehl, H., & Smith, G. F. (1959). 2,4,6-Tripyridyl-s-triazine as Reagent for Iron. Determination of Iron in Limestone, Silicates, and Refractories. *Analytical Chemistry, 31,* 1862-1867.

Contreras-Reyes, E., Jara, J., Grevemeyer, I., Ruiz, S., & Carrizo, D. (2012). Abrupt change in the dip of the subducting plate beneath north Chile. *Nature Geoscience, 5,* 342-345. doi: 10.1038/NGEO1447

D'Hondt, S. L., Jørgensen, B. B., Miller, D. J., et al. (2003). Proc. ODP, Init. Repts., 201. Ocean Drilling Program, College Station, TX.

Danovaro, R., Della Croce, N., Dell'Anno, A., & Pusceddu, A. (2003). A depocenter of organic matter at 7800m depth in the SE Pacific Ocean. *Deep-Sea Research I, 50,* 1411-1420. doi: 10.1016/j.dsr.2003.07.001

Dickens, G. R., Koelling, M., Smith, D. C., Schnieders, L. & IODP Expedition 302 Scientists (2007). Rhizon Sampling of Pore Waters on Scientific Drilling Expeditions: An Example from the IODP Expedition 302, Arctic Coring Expedition (ACEX). *Scientific Drilling, 4,* 22-25, doi: 10.2204/iodp.sd.4.08.2007

Egger, M., Riedinger, N., Mogollón, J. M., & Jørgensen, B. B. (2018). Global diffusive fluxes of methane in marine sediments. *Nature Geoscience, 11,* 421-426. doi: 10.1038/s41561-018-0122-8

Geersen, J., Ranero, C.R., Kopp, H., Behrmann, J. H., Lange, D., Klauke, I., Barrientos, S., Diaz-Naveas, J., Barckhausen, U., & Reichert, C. (2018a). Dies permanent extensional deformation in lower forearc slopes indicate shallow plate-boundary rupture. *Earth and Planetary Science Letters, 489,* 17-27. doi: 10.1016/j.epsl.2018.02.030

Geersen, J., Ranero, C.R., Klauke, I., Behrmann, J.-H., Kopp, H., Tréhu, A. M, Contreras-Reyes, E., Barckhausen, U., & Reichert, C. (2018b). Active Tectonics of the North Chilean Marine Forearc and Adjacent Oceanic Nazca Plate. *Tectonics, 37,* 4194-4211. doi: 10.1029/2018TC005087

Glud, R. N., Wenzhöfer, F., Middelboe, M., Oguri, K., Turnewitsch, R., Canfield, D. E., & Kitazato, H. (2013). High rates of microbial carbon turnover in sediments in the deepest oceanic trench on Earth. *Nature Geoscience, 6,* 284-288. doi: 10.1038/NGEO1773

Glud, R. N., Berg, P., Thamdrup, B., Larsen, M., Stewart, H. A., Jamison A. J., Glud, A., Oguri, K., Sanei, H., Rowden, A. A., & Wenzhöfer, F. (2021). Hadal trenches are dynamic hotspots for early diagenesis in the deep sea. *Communications Earth & Environment.* doi: 10.1038/s43247-020-00087-2

Hall, P. O. J., & Aller, R. C. (1992). Rapid small-volume flow-injection analysis for CO_2 and NH_4 in marine Sediments. *Limnology and Oceanography, 35,* 1113-1119. doi: 10.4319/lo.1992.37.5.1113

Heuer, V., et al. (2020). Temperature limits to deep subseafloor life in the Nankai Trough subduction zone. *Science, 370,* 1230–1234. doi: 10.1126/science.abd7934

Ichino, M. C., Clark, M. R., Drazen, J. C., Jamison, A., Jones, D. O. B., Martin, A. P., Rowden, A. A., Shank, T. M., Yancey, P. H., & Ruhl, H. A. (2015). The

distribution of benthic biomass in hadal trenches: A modelling approach to investigate the effect of vertical and lateral organic matter transport to the seafloor. *Deep-Sea Research I, 100,* 21-33. doi: 10.1016/j.dr.2015.01.010

Ikehara, K., Kanamatsu, T., Nagahashi, Y., Strasser, M., Fink, H., Usami, K., Irino, T., & Wefer, G. (2016). Documenting large earthquakes similar to the 2011 Tohoku-Oki earthquake from sediments deposited in the Japan Trench over the past 1500 years. *Earth and Planetary Science Letters, 445,* 48-56. doi: 10.1016/j.epsl.2016.04.009

Ikehara, K., Usami, K., & Kanamatsu, T. (2020). Repeated occurrence of surface-sediment remobilization along the landward slope of the Japan Trench by great earthquakes. *Earth, Planets and Space, 72,* 114. doi: 10.1186/s40623-020-01241-y

Inagaki, F., et al. (2015). Exploring deep microbial life in coal-bearing sediment down to ~2.5 km below the ocean floor. *Science, 349,* 420-424. doi: 10.1126/science.aaa6882

Inthorn, M., Wagner, T., Scheeder, G., & Zabel, M. (2006). Lateral transport controls distribution, quality and burial of organic matter along continental slopes in high-productivity areas. *Geology, 34,* 205-208. doi: 10.1130/G22153.1

Jamieson, A. J. (2015). The Hadal Zone: Life in the Deepest Oceans. Cambridge University Press, UK, pp. 382.

Kioka, A., Schwestermann, T., Moernaut, J., Ikehara, K., Kanamatsu, T., Eglinton, T. I., & Strasser, M. (2019a). Event Stratigraphy in a Hadal Oceanic Trench: The Japan Trench as Sedimentary Archive Recording Recurrent Giant Subduction Zone Earthquakes and Their Role in Organic Carbon Export to the Deep Sea. *Frontiers in Earth Science, 7,* 319. doi: 10.3389/feart.2019.00319

Kioka, A., Schwestermann, T., Moernaut, J., Ikehara, K., Kanamatsu, T., McHugh, C. M., dos Santos Ferreira, C., Wiemer, G., Haghipour, N., Kopf, A. J., Eglinton, T. I., & Strasser, M. (2019b). Megathrust earthquake drives drastic organic carbon supply to the hadal trench. *Scientific Reports., 9,* 1553. doi: 10.1038/s41598-019-38834-x

Kvenvolden, K. A., & McDonald, T. J. (1986). Organic geochemistry on the JOIDES Resolution—an essay. *Tech. Note 6*, 147 pp., Ocean Drill. Prog., Texas A&M Univ, College Station, Tex.

Loveless, J. P., & Meade, B. J. (2010). Geodetic imaging of plate motions, slip rates, and partitioning of deformation in Japan. *Journal of Geophysical Research, 115,* B02410. doi: 10.1029/2008JB006248

Luo, M., Gieskes, J., Chen, L., Shi, X., & Chen, D. (2017). Provenances, distribution, and accumulation of organic matter in the southern Mariana Trench rim and slope: Implication for carbon cycle and burial in hadal trenches. *Marine Geology, 386,* 98-106. doi: 10.1016/j.margeo.2017.02.012

Luo, M., Glud, R. N., Pan, B., Wenzhöfer, F., Xu, Y., Lin, G., & Chen, D. (2018). Benthic Carbon Mineralization in Hadal Trenches: Insights From In Situ Determination of Benthic Oxygen Consumption. *Geophysical Research Letters, 45,* 2752–2760. doi: 10.1002/2017GL076232

McHugh, C. M., Seeber, L., Braudy, N., Cormier, M.-H., Davis, M. B., Diebold, J. B., Dieudonne, N., Douilly, R., Gulick, S. P. S., Hornbach, M. J., Johnson III, H. E., Ryan Mishkin, K., Sorlien, C. C., Steckler, M. S., Symithe, S. J., & Templeton, J. (2011). Offshore sedimentary effects of the 12 January 2020 Haiti earthquake. *Geology, 39,* 723-726. doi: 10.1130/G31815.1

McHugh, C. M., Kanamatsu, T., Seeber, L., Bopp, R., Cormier, H.-M., & Usami, K. (2016). Remobilization of surficial slope sediment triggered by the A.D. 2011 M_W 9 Tohoku-Oki earthquake and tsunami along the Japan Trench. *Geology, 44,* 391-394. doi: 10.1130/G37650.1

McHugh, C. M., Seeber, L., Rasbury, T., Strasser, M., Kioka, A., Kanamatsu, T., Ikehara, K., & Usami, K. (2020). Isotopic and sedimentary signature of megathrust ruptures along the Japan subduction margin. *Marine Geology, 428,* 106283. doi: 10.1016/j.margeo.2020.106283

Muñoz, P., Lange, C.B., Gutiérrez, D., Hebbeln, D., Salamanca, M. A., Dezileau, L., Reyss, J. L., & Benninger, L. K. (2004). Recent sedimentation and mass accumulation rates based on ^{210}Pb along the Peru–Chile continental margin. *Deep-Sea Research II, 51,* 2523–2541. doi: 10.1016/j.dsr2.2004.08.015

Niggemann, J., Ferdelman, T. G., Lomstein, B. A., Kallmeyer, J., & Schubert, C.J. (2007). How depositional conditions control input, composition, and degradation of organic matter in sediments from the Chilean coastal upwelling region. *Geochimica et Cosmochimica Acta, 71*, 1513-1527. doi: 10.1016/j.gca.2006.12.012

Oguri, K., Kawamura, K., Sakaguchi,A., Toyofuku, T., Kasaya, I., Murayama, M., Fujikura, K., Glud, R. N., & Kitazato, H. (2013). Hadal disturbance in the Japan Trench induced by the 2011 Tohoku-Oki earthquake. *Scientific Report, 3:1915.* doi:10.1038/srep01915

Oguri, K., Turnewitsch, R., Masqué, P., Zabel, M., Stewart, H.A., Stehlikova, J., MacKinnon, G., Rowden, A., Wenzhöfer, F., & Glud, R.N. (in rev.) Sedimentation Accumulation and Carbon Burial in Four Hadal Trench Systems. *Biogeosciences.*

Pape, T., Bahr, A., Rethemeyer, J., Kessler, J. D., Sahling, H., Hinrichs, K-.U., Klapp, S. A., Reeburgh, W. S., & Bohrmann, G. (2010). Molecular and isotopic partitioning of low-molecular weight hydrocarbons during migration and gas hydrate precipitation in deposits of a high-flux seepage site. *Chemical Geology, 269,* 350-363. doi: 10.1016/j.chemgeo.2009.10.009

Polonia, A., Panieri, G., Gasperini, L., Gasparotto, G., Bellucci, L. G., & Torelli, L. (2013). Turbidite paleoseismology in the Calabrian Arc Subduction Complex

(Ionian Sea). *Geochemistry, Geophysics, Geosystems, 14,* 112–140. doi: 10 .1029 /2012GC004402.

Riedinger, N., Kasten, S., Gröger, J., Franke, C., & Peifer, K. (2006). Active and buried authigenic barite fronts in sediments from the Eastern Cape Basin. *Earth and Planetary Science Letters, 241,* 876–887. doi: 10.1016/j.epsl.2005.10.032

Salazar, D. et al. (2022) Did a 3800-year-old M_W~9.5 earthquake trigger major social disruption in the Atacama Desert? *Science Advances*, doi: 10.1126/scladv.abm2996

Schurrr, B., Asch, G., Hainzl, S., Bedford, J., Hoechner, A., Palo, M., Wang, R., Moreno, M., Bartsch, M., Zhang, Y., Oncken, O., Tilmann, F., Dahm, T., Victor, P., Barrientos, S., & Vilotte, J.-P. (2014). Gradual unlocking of plate boundary controlled initiation of the 2014 Iquique earthquake. *Nature, 512.* doi: 10.1038/nature13681

Schwestermann, T., Huang, J., Konzett, J., Kioka, A., Wefer, G., Ikehara, K., Moernaut, J., Eglinton, T. I., & Strasser, M. (2020). Multivariate Statistical and Multiproxy Constraints on Earthquake-Triggered Sediment Remobilization Processes in the Central Japan Trench. *Geochemistry, Geophysics, Geosystems, 21.* doi: 10.1029/2019GC008861

Schwestermann, T., Eglinton, T. I.; Haghipour, N., McNichol, A. P., Ikehara, K.; & Strasser, M. (2021). Event-dominated transport, provenance, and burial of organic carbon in the Japan Trench. *Earth and Planetary Science Letters, 563,* 116870. doi: 10.1016/j.epsl.2021.116870.

Seiter, K., Hensen, C., Schröter, J., & Zabel, M. (2004) Organic carbon content in surface sediments – defining regional provinces. *Deep-Sea Res. I*, 51:2001-2026.

Strasser, M., Kölling, M., dos Santos Ferreira, C., Fink, H. G., Fujiwara, T., Henkel, S., Ikehara, K., Kanamatsu, T., Kawamura, K., Kodaira, S., Römer, M., & Wefer, G. (2013). A slump in the trench: Tracking the impact of the 2011 Tohoku-Oki earthquake. *Geology, 41,* 935-938. doi: 10.1130/G34477.1

Strasser, M. et al. (2017). Report and preliminary results of R/V SONNE cruise SO251, Extreme events Archived in the GEological Record of Japan's Subduction margins (EAGER-Japan), Leg A SO251-1, Yokohama - Yokohama, 04.10.2016 – 15.10.2016, Leg B SO251-2, Yokohama - Yokohama, 18.10.2016 – 02.11.2016. *Berichte, MARUM – Zentrum für Marine Umweltwissenschaften, Fachbereich Geowissenschaften, Universität Bremen, No. 318*, 217 pages. Bremen. ISSN 2195-9633.

Thamdrup, B., Schauberger, C., Larsen, M., Trouche, B., Maignien, L., Arnaud-Haond, S., Wenzhöfer, F., & Glud, R. N. (2021). Anammox bacteria drive fixed nitrogen loss in hadal trench sediments. *Proceedings of the National Academy of Science, 118.* doi: 10.1073/pnas.2104529118.

Turnewitsch, R., Falahat, S., Stehlikova, J., Oguro, K., Glud, R. N., Middelboe, M., Kitazato, H., Wenzhöfer, F., Ando, K., Fujio, S., & Yanagimoto, D. (2014). Recent sediment dynamics in hadal trenches: Evidence for the influence of higher-frequency (tidal, near-inertial) fluid dynamics. *Deep-Sea Research I, 90,* 125-138. doi: 10.1016/j.dsr.2014.05.005

van Haren, H. (2020). Challenger Deep internal wave turbulence events. *Deep-Sea Research I*, 103400. doi: 10.1016/j-dsr.2020.103400

Wakeham, S. (2002). Diagenesis of Organic Matter at the Water-Sediment Interface. In: Gianguzza, A., Pelizzetti, E., & Sammartano, S. (eds) *Chemistry of Marine Water and Sediments*, Springer, 147-164, doi: 10.1007/978-3-662-04935-8_6.

Wefer, G. et al. (2014). Report and preliminary results of R/V SONNE Cruise SO219A, Tohoku-Oki Earthquake – Japan Trench, Yokohama – Yokohama, 08.03.2012 – 06.04.2012. *Berichte, MARUM – Zentrum für Marine Umweltwissenschaften, Fachbereich Geowissenschaften, Universität Bremen, No. 301*, 83 pp. Bremen. ISSN 2195-9633.

Wenzhöfer, F., Oguri, K., Middelboe, M., Turnewitsch, R., Toyofuku, T., Kitazato, H., & Glud, R. N. (2016). Benthic carbon mineralization in hadal trenches: Assessment by in situ O2 microprofile measurements. *Deep-Sea Research I, 116,* 276-286. doi: 10.1016/j.dsr.2016.08.013

Wenzhöfer, F. (2019). The Expedition SO261 of the Research Vessel SONNE to the Atacama Trench in the Pacific Ocean in 2018. *Reports on Polar and Marine Research No. 729*, 111 pages. doi: 10.2312/BzPM_0729_2019

Xu, Y., Li, X., Luo, M., Xiao, W., Fang, F., Rashid, H., Peng, Y., Li, W., Wenzhöfer, F., Rowden, A. A., & Glud, R. N. (2021). Distribution, Source, and Burial of Sedimentary Organic Carbon in Kermadec and Atacama Trenches. *Journal of Geophysical Research Biogeosciences*. doi: 10.1029/2020JG006189

Yokota, Y., Koketsu, K., Fujii, Y., Satake, K., Sakai, S. I., Shinohara, M., & Kanazawa, T. (2011). Joint inversion of strong motion, teleseismic geodetic, and tsunami datasets for the rupture process of the 2011 Tohoku earthquake: *Geophysical Research Letters, 38,* L00G21. doi: 10.1029/2011GL050098.

Zhuang, G.-C., Heuer, V. B., Lazar, C. S., Goldhammer, T., Wendt, J., Samarkin, V. A., Elvert, M., Teske, A. P., Joye, S. B., & Hinrichs, K.-U. (2018). Relative importance of methylotrophic methanogenesis in sediments of the Western Mediterranean Sea. *Geochimica et Cosmochimica Acta, 224,* 171–186. doi: 10.1016/j.gca.2017.12.024

Figures and Tables

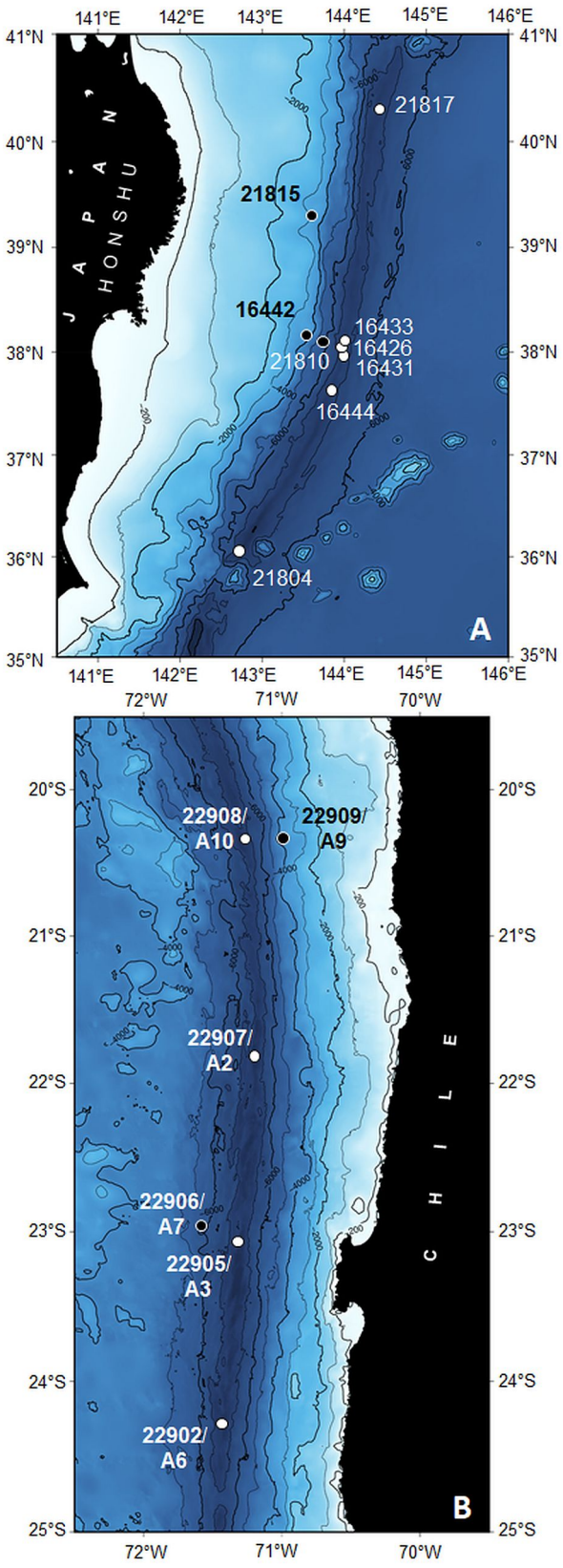
141°E
142°E
143°E
144°E
145°E
146°E
41°N
40°N
39°N
38°N
37°N
36°N
35°N
JAPAN
HONSHU
21817
21815
16442
16433
16426
21810
16431
16444
21804
A
72°W
71°W
70°W
20°S
21°S
22°S
23°S
24°S
25°S
22908/
A10
22909/
A9
22907/
A2
22906/
A7
22905/
A3
22902/
A6
CHILE
B

Fig. 1.

Overview maps of the Japan Trench (East of Honshu) (A) and the Atacama Trench (West of Chile) (B). Core locations along the trench axes are marked in white. Coring sites on the accompanying continental rise and the abyssal plains are marked in black.

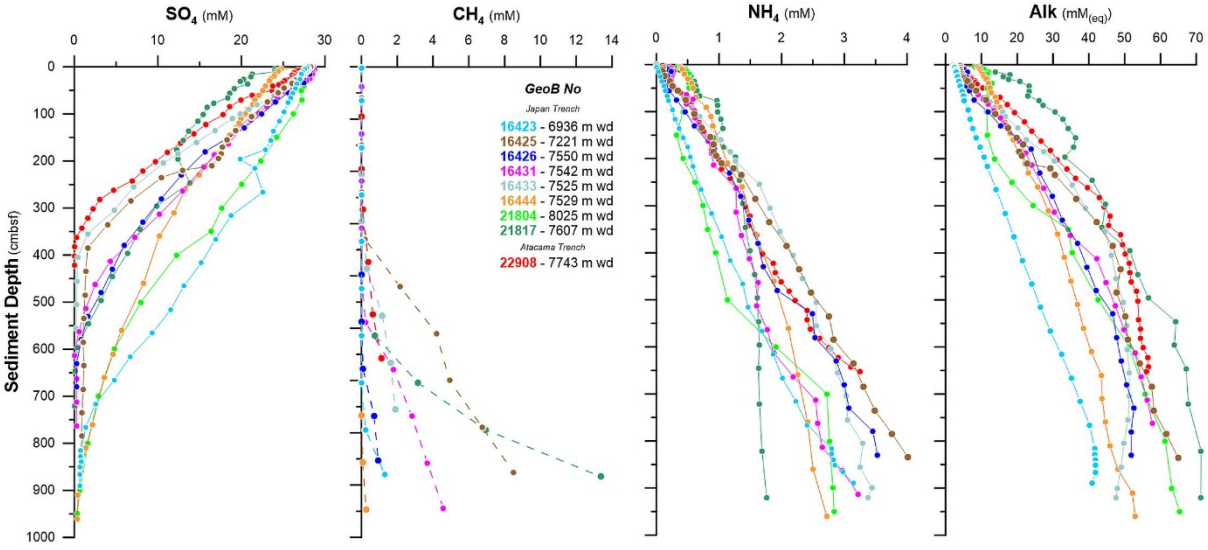

Fig. 2.

Pore water profiles of sulfate, methane and ammonia concentrations and alkalinity in nine sediment cores recovered from trench-fill basins off Japan and Chile showing clear sulfate methane transition zones only few meters below the seafloor. Due to the outgassing of the sediments caused by the strong pressure decrease during their long transport from the seafloor to the surface, the analyzed methane concentrations certainly do not correspond to the in-situ CH_4 concentrations. $^{13}CH_4$ values around –91 ‰ (V-PDB) in core GeoB22908-2(A10) clearly indicate a microbial origin of methane in the course of CO_2 reduction deeper in the sediment.

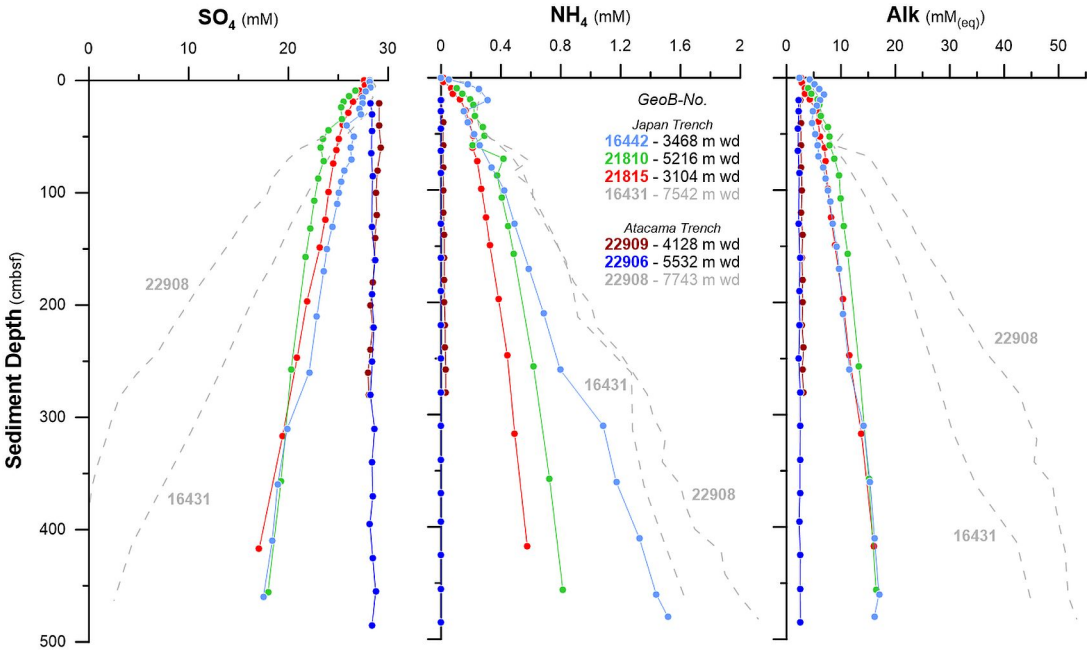

Fig. 3.

Pore water profiles of sulfate and ammonium concentrations and alkalinity from sites at trench flanks or from the oceanward abyssal plain (GeoB22906/A7). For comparison, profiles from cores recovered in along the trench axes are shown in grey (cf. Fig. 2).

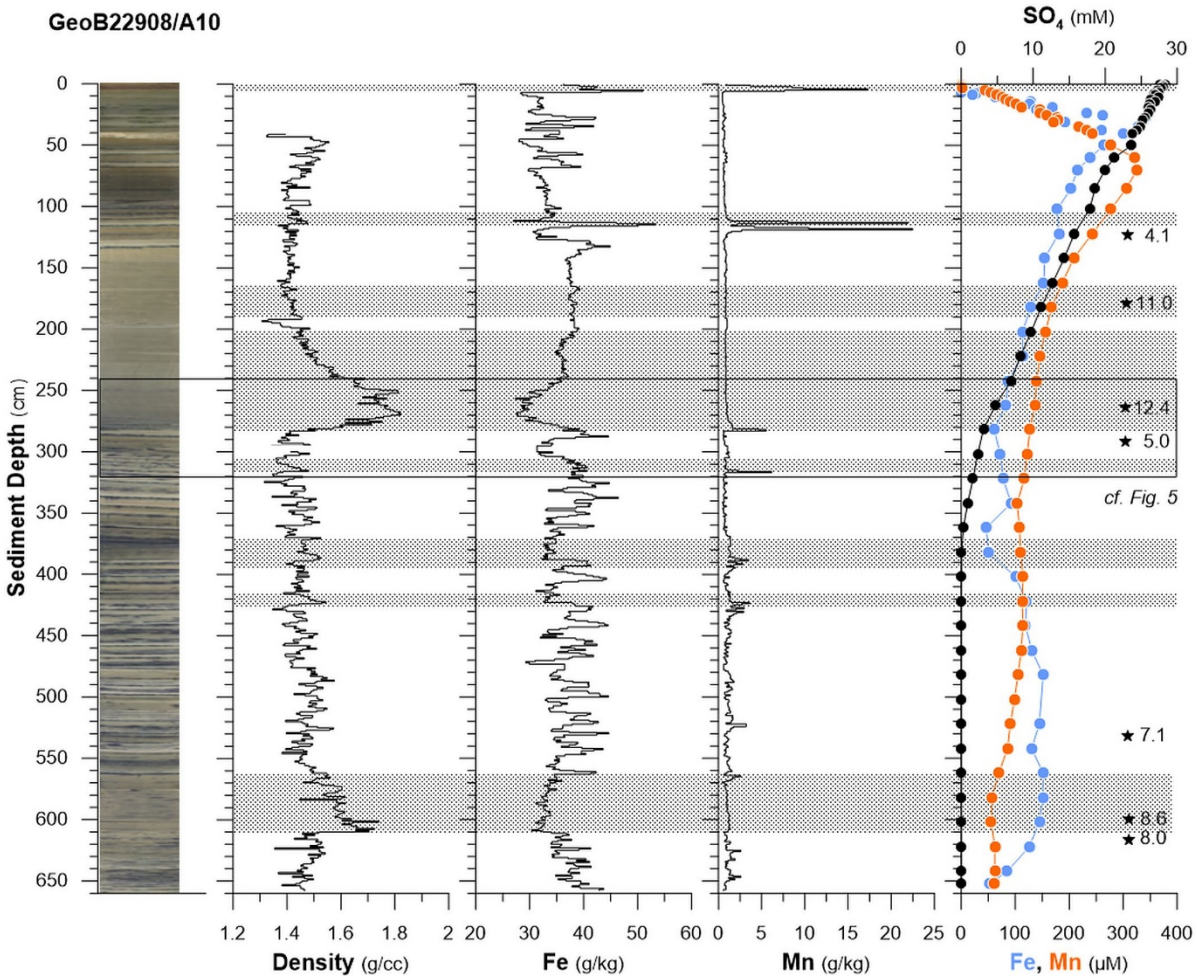

Fig. 4.

★Logging data from Atacama Trench core GeoB22908-2(A10). The profile of gamma ray density clearly shows two thick turbidite layers (grey shaded) whose lower edges are at about 285 cmbsf and 611 cmbsf. In addition, typical enrichments of the redox sensitive elements iron and manganese as well as the color changes in color scan indicate a large number of smaller mass wasting events. The AMS^{14}C dating ( ) also proves the alternating deposits. The pore water gradients of Fe and Mn show that significant microbially catalyzed reductions occur only within the first meter.

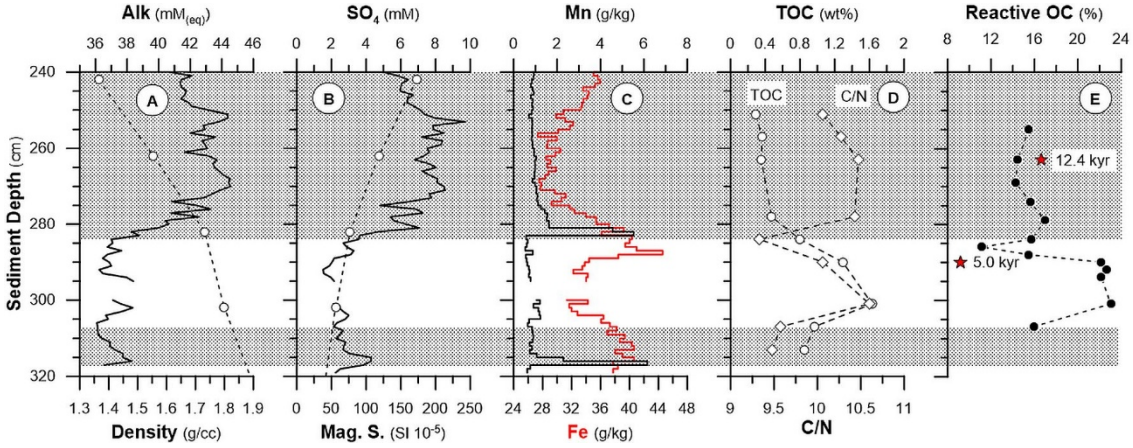

Fig. 5.

Detailed view of measured data in a section of sediment core GeoB22908-2(A10) from the trench axis in the Atacama Trench. All analytical data (density, magnetic susceptibility, Mn, Fe, TOC, C/N, $^{14}C_{TOC}$ and reactive organic carbon) prove that the upper and lower part of this section is attributable to bulk redepositions (turbidites) which features that are clearly different from the material of the layer in between. Of particular importance is that the hemipelagic interlayer not only has a higher total organic carbon content (D) but the amount of reactive material in it is also significantly higher (E). The accumulations of iron and especially the prominent manganese peaks are the known products of sudden sedimentation events.

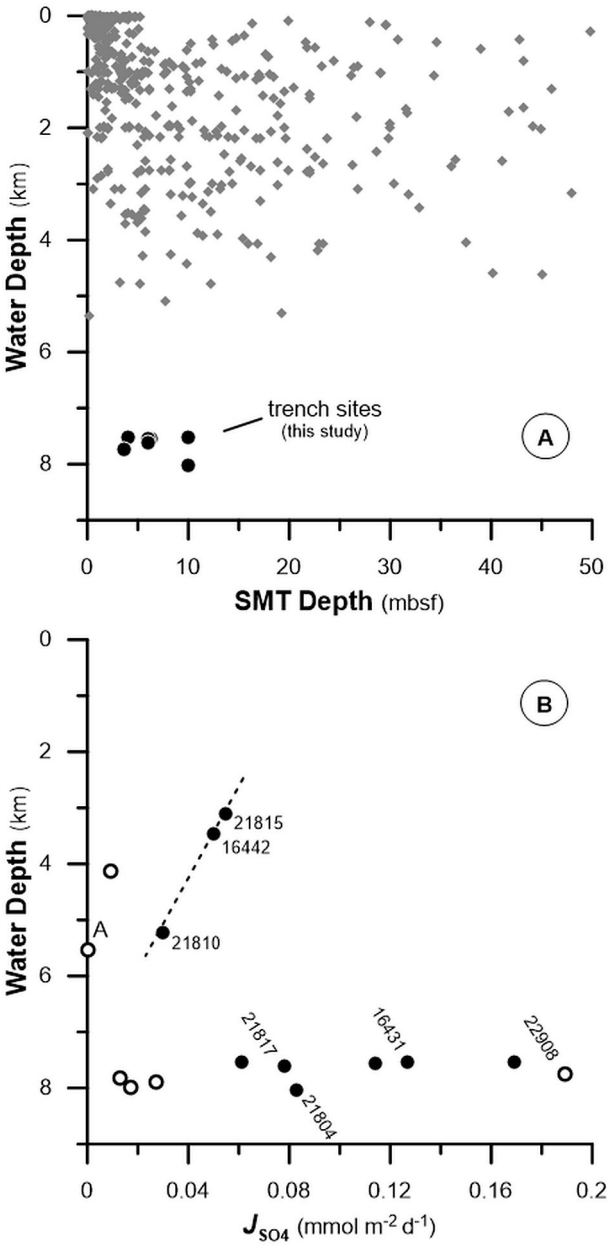

Fig. 6.

Upper graph: SMT depths versus water depths. Despite large water depths, the SMT is no deeper than 10 mbsf at 7 of 10 sites in the trench axes. Grey diamonds: global data compilation (Egger et al., 2018).

Lower graph: Rates of diffusive SO_4^{2-}-fluxes plotted versus the water depths of

respective sites (Japan Trench: , Atacama Trench:). In both hadal zones, the flux rates are clearly higher than on the flanks of the trenches or on the oceanward abyssal plain (A). Sediment cores from flank sites in the Japan Trench (GeoB16442, 21810 and 21815) further suggest that the classic sequence of decreasing flow rates with increasing water depth is evident here.

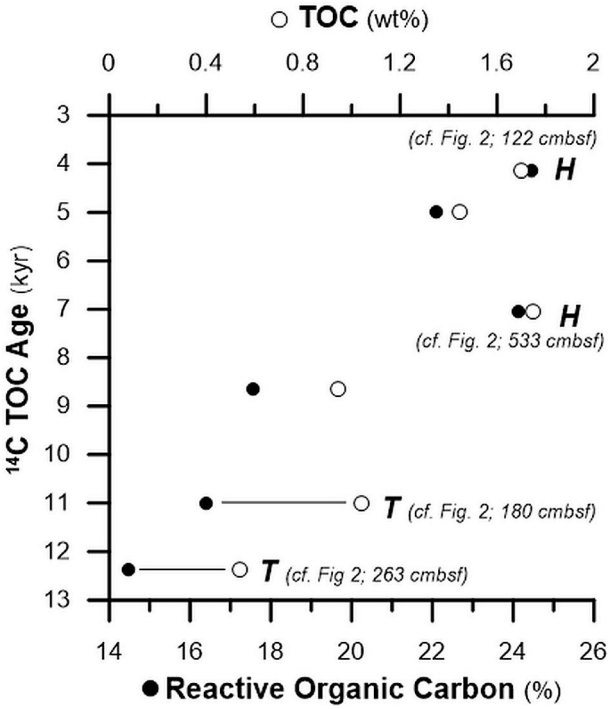

Fig. 7.

Relationship between the age of sediment samples at the trench axis site GeoB22908/A10 in the Atacama Trench, the respective TOC and the fractions of reactive microbially degradable carbon contained therein. The trend of decreasing TOC with age is likely to be due to changes in primary input rather than microbial degradation of organic debris. Much more significant is the documentation that the reactive fraction of organic carbon in redeposited material (T) is significantly lower than in "normally" sedimented layers (H).

Table 1

Sampling sites with position, water depth and references of already published information about the respective sites. (T: trench axes; R: continental rise; A: abyssal plain)

Cruise	**GeoB-No**	**Site**	**T/R/A**	**Latitude**	**Longitude**	depth
	Core length (m)	**Ref.**				

	Japan Trench							
SO219A	16426-1		T	38°04.228'N	143°58.975'E	7.550	8.39	a
	16431-1		T	38°00.177'N	143°59.981'E	7.542	9.40	b, c, d, e
	16433-1		T	38°07.843'N	144°00.135'E	7.525	9.26	b
	16442-1		R	38°11.467'N	143°33.249'E	3.468	4.85	---
	16444-1		T	37°42.017'N	143°52.377'E	7.529	11.38	b, d
SO251	21804-2		T	36°04.256'N	142°44.045'E	8.025	9.76	d, e, f
	21810-1		R	38°06.787'N	143°41.662'E	5.216	4.26	f
	21815-1		R	39°19.575'N	143°38.874'E	3.104	4.67	f
	21817-1		T	40°23.735'N	144°25.256'E	7.607	9.71	d, e, f
	Atacama Trench							
SO261	22902-1	A2	T	24°17.044'S	071°25.403'W	7.832	4.00	g, h
	22905-2	A3	T	23°03.140'S	071°18.165'W	7.996	3.40	g, h, i
	22906-2	A7	A	22°57.259'S	071°37.245'W	5.532	8.55	g, h, i
	22907-2	A2	T	21°47.311'S	071°12.275'W	7.898	5.67	g, h
	22908-2	A10	T	20°19.574'S	071°17.551'W	7.743	6.58	g, h, i
	22909-1	A9	R	20°21.090'S	070°59.399'W	4.128	2.80	g, h

Table 2

Diffusive flux rates (J) of sulfate and methane as calculated from pore water profiles. (T: trench; R: continental rise; A: abyssal plain)

GeoB-No	**Site**	**T/R/A**	**Water depth**	$\boldsymbol{J_{SO4}}$	$\boldsymbol{J_{CH4}}$
			(m)	(mmol m^{-2} d^{-1})	(mmol m^{-2} d^{-1})
Japan Trench					
16426-1		T	7,550	0.089±0.009	0.017±0.002
16431-1		T	7,542	0.099±0.010	0.030±0.003
16433-1		T	7,525	0.132±0.013	0.024±0.002
16444-1		T	7,529	0.048±0.005	0.009±0.001
21804-2		T	8,025	0.065±0.007	0.002±0.000
21817-1		T	7,607	0.061±0.006	0.066±0.007
16442-1		R	3,468	0.039±0.004	---
21810-1		R	5,216	0.023±0.002	---
21815-1		R	3,104	0.043±0.004	---
Atacama Trench					
22902-1	A6	T	7,832	0.010±0.001	---
22905-2	A3	T	7,996	0.013±0.001	---
22907-2	A2	T	7,898	0.021±0.002	---
22908-2	A10	T	7,743	0.148±0.015	0.008±0.001
22909-1	A9	R	4,128	0.007±0.001	---
22906-2	A7	A	5,532	0.000±0.000	---

GeoB-No	Site	T/R/A	Water depth	J_{SO4}	J_{CH4}
global average data					
(after Egger et al., 2018)					
outer shelf	50 – 200	0.230	---		
continental slope	200 – 2,000	0.078	---		
continental rise	2,000 – 3,500	0,007	---		
Abyss	>3,500	0.004	---		